

■ Full-Length Paper ■ By a grant from Research Institute for Integrated Science, Kanagawa University

## Crystallization of Amorphous Si Layer Assisted by Quantum Beam Irradiation Studied by Rutherford Backscattering Channeling Method

Yasushi Hoshino<sup>1,2,3</sup> and Jyoji Nakata<sup>1,2</sup>

<sup>1</sup> Department of Mathematics and Physics, Faculty of Science, Kanagawa University, Hiratsuka City, Kanagawa 259-1293, Japan

<sup>2</sup> Research Institute for Integrated Science, Kanagawa University, Hiratsuka City, Kanagawa 259-1293, Japan

<sup>3</sup> To whom correspondence should be addressed: E-mail: yhoshino@kanagawa-u.ac.jp

**Abstract:** We investigated the crystallization of an amorphous Si layer grown on single crystalline Si substrates enhanced by irradiation with various energetic particles. We comprehensively compared the crystallization rate on 150-keV proton beam irradiation with that on 8-MeV electron beam irradiation under the same condition of displaced atom density to examine the effect of inelastic energy deposition on crystallization, since the electronic energy loss in Si for a 150-keV proton is significantly different from that for an 8-MeV electron. The crystallization rate was quantitatively analyzed by the Rutherford backscattering channeling method. Consequently, recrystallization of the amorphous Si layer was only observed in the case of proton beam irradiation. We proposed some factors to explain the beam induced crystallization process observed with high-energy proton and electron irradiation.

**Keywords:** ion beam induced epitaxial crystallization, electron beam induced epitaxial crystallization, nuclear energy deposition, electronic energy deposition, Rutherford backscattering spectroscopy

### Introduction

Quantum beam irradiation is one of the essential techniques for fabrication of functional materials as well as characterization of material properties. It is well recognized that ion implantation has in particular succeeded in highly controlled selective impurity doping in materials and widely applied to fabrication of semiconductor devices today. It is previously reported that annealing under ion beam irradiation enhances the epitaxial crystallization of amorphous Si layer synthesized on a single crystalline Si substrate at low substrate temperatures at which the crystallization could not take place by conventional annealing under thermal equilibrium condition<sup>1-9)</sup>. Such an epitaxial crystallization at low temperatures was also observed in electron beam irradiation so far<sup>10-13)</sup>. Here, beam induced epitaxial crystallization by ion and electron beam is respectively known as IBIEC (ion beam induced epitaxial crystallization) and EBIEC (electron beam induced epitaxial crystallization). Here, the energy deposition process

from energetic particles to lattice system is categorized into two contributions of inelastic energy deposition of electron excitation/ionization and elastic energy deposition by direct collision between incident and target nuclei. It has been widely recognized that the creation of vacancies and interstitials induced by elastic collisions primarily plays the most important role in the beam induced crystallization processes. Some researchers however pointed out that the electron-hole pairs generated by electronic energy deposition due to inelastic scattering also greatly contribute to the enhancement of recrystallization, though the reliable verification on the role of inelastic energy deposition in the recrystallization process has not been found yet<sup>14-17)</sup>. To clarify the recrystallization mechanism, the irradiation of different types of energetic particles, which provide different energy deposition and defect formation in a lattice system, should be valuable.

We performed EBIEC and IBIEC treatments to

amorphized Si(100) samples at 400°C, and compared the results under the same conditions of substrate temperature and the nucleation density of displaced atom. We comprehensively investigated EBIEC and proton-IBIEC, in which the electronic energy loss is predominant process in ion-solid interactions rather than nuclear energy loss, and discuss the role of inelastic energy deposition in the radiation enhanced crystallization.

## Materials and Methods

We prepared a 4-inch *n*-type Si(100) (1-10 Ω cm) wafer and cleaved it to small 6×6 mm<sup>2</sup> pieces. These samples were then self-irradiated by 190-keV Si<sup>+</sup> ions with ion fluences of 2.0×10<sup>15</sup> and 5.0×10<sup>15</sup> cm<sup>-2</sup> at room temperature (RT) to form surficial amorphous Si layer.

Electron beam irradiation was performed by electron linear accelerator (LINAC) facility at the Institute for Integrated Radiation and Nuclear Science, Kyoto University. Pulsed electron beam of 8-MeV energy was irradiated to the samples at the substrate temperature of 400°C with a beam fluence of 4.2×10<sup>19</sup> cm<sup>-2</sup> in He gas ambient. The irradiation time was about 46 h. The fluence was determined so that the atomic displacement density of 4.5×10<sup>20</sup> cm<sup>-3</sup> (~0.01 dpa: displacement per atom) coincides with that in the previous neutron irradiation experiments<sup>18)</sup>. Here, the cross section for atomic displacement of Si in irradiation of 8-MeV electron was obtained by interpolation in numerically calculated values reported by Oen, to be about 3×10<sup>-22</sup> cm<sup>2</sup><sup>19)</sup>. The sample temperature was monitored by K-type thermocouples contacting the back-surface of samples via an ultra-thin mica film. During the EBIEC treatment, we carefully adjusted the beam current and air flow intensity of a blower set outside the irradiation chamber to keep the substrate temperature at 400°C.

To substantially distinguish the crystallization by electron beam irradiation from that by the thermal effect, we annealed another piece of amorphized samples in a conventional electrical furnace in He ambient without beam irradiation at the same temperature and durations as the conditions of EBIEC treatments.

Ion irradiation was carried out with a 200-kV medium-current ion implanter at Shonan Hirat-

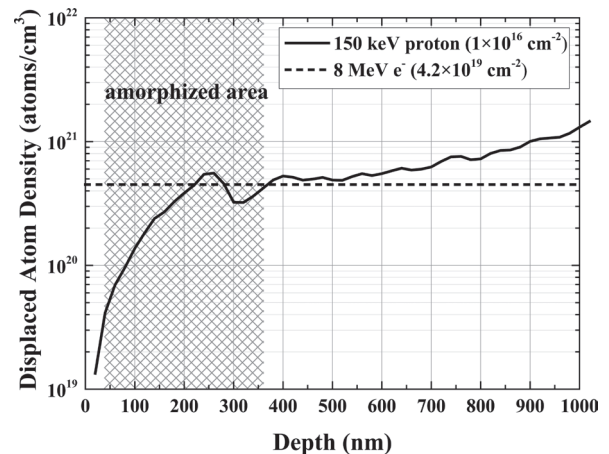


Fig. 1. The atomic displacement density for 150-keV proton and 8-MeV electron with the respective fluences of  $1.0 \times 10^{16}$  and  $4.2 \times 10^{19}$  cm<sup>-2</sup> as a function of depth.

suka Campus, Kanagawa University. The proton beam with an incident energy of 150-keV was irradiated at 400°C with a fluence of  $1 \times 10^{16}$  cm<sup>-2</sup>. The beam flux was  $\sim 2 \times 10^{11}$  cm<sup>-2</sup> s<sup>-1</sup>. According to TRIM Monte-Carlo simulation<sup>20)</sup>, the atomic displacement density around the interesting region with a fluence of  $1.0 \times 10^{16}$  cm<sup>-2</sup> is estimated to be  $4.5 \times 10^{20}$  cm<sup>-3</sup>, which is comparable to that by the EBIEC treatment of  $4.2 \times 10^{19}$  cm<sup>-2</sup> fluence. The atomic displacement density for 150-keV proton and 8-MeV electron with the respective fluences of  $1.0 \times 10^{16}$  and  $4.2 \times 10^{19}$  cm<sup>-2</sup> as a function of depth is shown in Fig. 1. In order to evaluate the actual IBIEC effect on recrystallization, we covered half area of the sample surface with another small Si piece; accordingly, the masked area can be a good monitor for thermal annealing effect at 400°C without beam irradiation.

The crystallized thickness and quality of irradiated

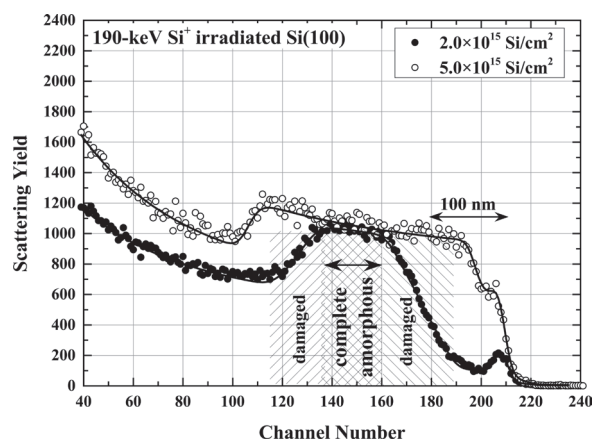


Fig. 2. RBS-channeling spectra for prepared as-amorphized specimens by self-bombardment with  $2 \times 10^{15}$  and  $5 \times 10^{15}$  cm<sup>-2</sup> fluences.

area were analyzed by Rutherford backscattering (RBS) channeling method using 2.0 MeV  $\text{Li}^{2+}$  projectiles at the scattering angle of  $120^\circ$ .

Figure 2 shows RBS-channeling spectra for prepared as-amorphized specimens by self-bombardment with  $2 \times 10^{15}$  and  $5 \times 10^{15} \text{ cm}^{-2}$  fluences. It is clearly found in RBS spectrum for the as-amorphized sample with  $2.0 \times 10^{15} \text{ cm}^{-2}$  fluence that an embedded amorphous Si layer with  $\sim 100 \text{ nm}$  (Fig. 2A) width was sandwiched with damaged Si layers. After the  $\text{Si}^+$  irradiation of  $5.0 \times 10^{15} \text{ cm}^{-2}$  fluence, the embedded amorphous region grew significantly toward the surface and deeper substrate, though very thin surface and interface regions were not completely amorphized and remained as damaged layers, probably consisting of amorphous-like structure incorporating small crystalline Si grains.

## Results

Figure 3 shows RBS-channeling spectra for the samples of as-amorphized (red), EBIEC (green), and furnace-annealed (blue) for different self-bombarded samples with Si fluences of (A)  $2.0 \times 10^{15}$  and (B)  $5.0 \times 10^{15} \text{ cm}^{-2}$ . As clearly seen in the spectra with green

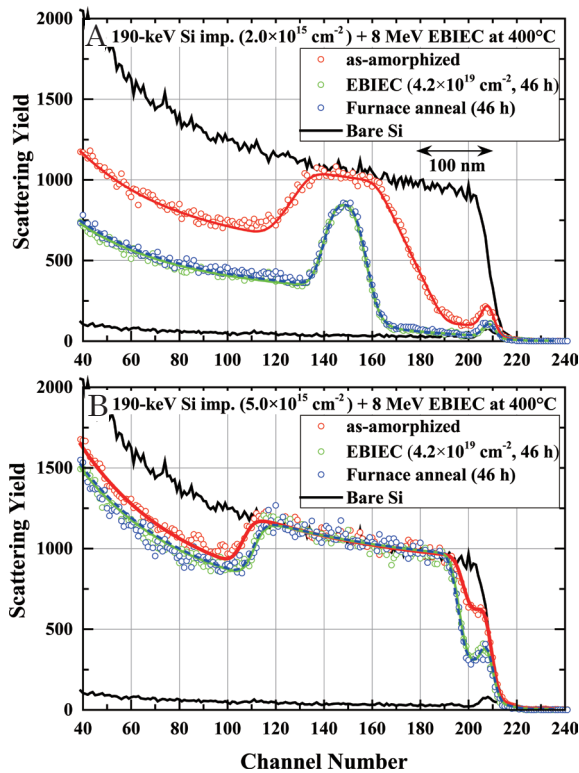


Fig. 3. RBS-channeling spectra for the samples of as-amorphized (red), EBIEC (green), and furnace-annealed (blue) at  $400^\circ\text{C}$  for different self-bombarded samples with Si fluences of (A)  $2.0 \times 10^{15}$  and (B)  $5.0 \times 10^{15} \text{ cm}^{-2}$ .

and blue colors depicted in Fig. 3A, the recrystallization took place from both sides of the upper and deeper interfaces by EBIEC as well as by FA treatment. The recrystallization rate was however significantly slow down near the embedded complete amorphous layer. The remarkable difference in the crystallization between EBIEC and FA treatments was not confirmed. The observed recrystallization was therefore attributed to only the thermal effect at  $400^\circ\text{C}$  temperature. In Fig. 3B, the crystallization in thin damaged layer existing very near the surface and the deeper interface was observed by both EBIEC and FA treatments, but the crystallization almost stopped in front of the complete amorphous region. The *a/c* interfaces did not move even though the fluence further increased. Small crystalline grains remaining in the heavily damaged regions are presumably involved in the recrystallization. Consequently, the significant enhancement of the crystallization of amorphized Si layer by EBIEC treatment was not clearly confirmed in the annealing treatments at  $400^\circ\text{C}$ .

We next show the effect of IBIEC treatment by 150 keV proton irradiation on the recrystallization of

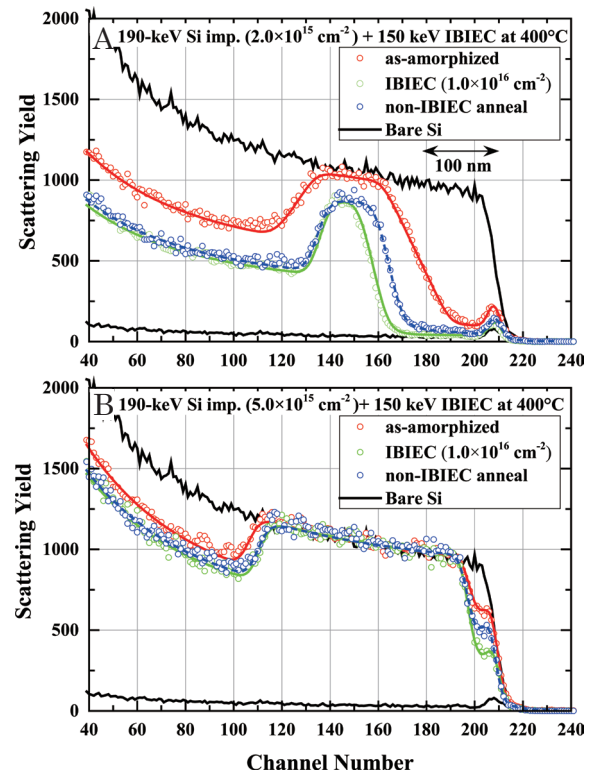


Fig. 4. RBS-channeling spectra for the samples of as-amorphized (red), proton-IBIEC (green), and furnace-annealed (blue) at  $400^\circ\text{C}$  for different self-bombarded samples with Si fluences of (A)  $2.0 \times 10^{15}$  and (B)  $5.0 \times 10^{15} \text{ cm}^{-2}$ .

amorphous Si layer embedded in Si(100) substrates synthesized by self-bombardment. Figure 4 shows RBS-channeling spectra for the samples of as-amorphized (red), proton-IBIEC (green), and furnace-annealed (blue) for different self-bombarded samples with Si fluences of (A)  $2.0 \times 10^{15}$  and (B)  $5.0 \times 10^{15}$   $\text{cm}^{-2}$ . The crystallization by non-IBIEC annealing was almost stopped in front of the embedded amorphous region (see blue curve), as already observed in the EBIEC samples shown in Fig. 3. It is found on the other hand that the recrystallization by proton IBIEC treatment progressed from the upper *c/a* interface overcoming the depth near which the crystallization stopped for the non-IBIEC sample (compare green curve to blue one). The front *c/a* interface moved toward deeper direction as further increasing IBIEC fluence by proton, which was not observed in the EBIEC treatments. After  $\text{Si}^+$  irradiation of  $5.0 \times 10^{15}$   $\text{cm}^{-2}$  fluence, the recrystallization took place from the damaged region located near both deeper and shallower *a/c* interfaces, as already mentioned in EBIEC and FA samples (Fig. 3). In the deeper damaged layer, recrystallization proceeded up to the amorphous region, but completely stopped in front of the complete amorphous region ( $\sim 350$  nm depth). In the shallower damaged layer ( $< 40$  nm depth), the recrystallization was initially developed laterally and then vertically proceeded. It is consequently suggested that ion beam irradiation significantly assists the epitaxial recrystallization.

## Discussion

As described above, electron beam irradiation did not show annealing effect of amorphous Si. However, proton beam annealing effectively enhanced the epitaxial recrystallization. As already mentioned in Fig. 1, the atomic displacement density around the focused depth region generated by H-irradiation of  $1.0 \times 10^{16}$   $\text{cm}^{-2}$  fluence was estimated to be  $4.5 \times 10^{20}$   $\text{cm}^{-3}$ , which is comparable to that by EBIEC treatment of  $4.2 \times 10^{19}$   $\text{cm}^{-2}$  fluence.

The electronically deposited energy (A) and the total number of created electron-hole pairs (B) by 150-keV proton ( $1 \times 10^{16}$   $\text{cm}^{-2}$ ) and 8-MeV electron ( $4.2 \times 10^{19}$   $\text{cm}^{-2}$ ) in Si are shown in Fig. 5. The data for proton was referred from SRIM table<sup>20)</sup> and those for electron was from a data table edited by Berger and Seltzer<sup>21)</sup>. Here, the two contributions of energy

transfer from high-energy electron beam: direct collision and Bremsstrahlung were considered, though 8-MeV electrons employed in this study predominantly lose the kinetic energy via the direct collision processes of electron excitation and ionization. The inelastic energy loss of 150-keV proton and 8-MeV electron in Si material is thus estimated to be about 100 eV/nm and 0.4 eV/nm, respectively. It is clearly found that total electron-hole pairs by the electron beam irradiation is about one order higher than those by proton beam irradiation, indicating that large energy deposition by inelastic effect from 8-MeV electron is more expected. As shown in Figs. 4 and 5, however, the enhancement of recrystallization was not observed for the EBIEC process, suggesting that the recrystallization occurred in the IBIEC process cannot be demonstrated by only inelastic energy effect. We thus consider possible three factors for accounting for observed results. It is firstly known that electron beam irradiation to Si did not form collision cascade, resulting in differ-

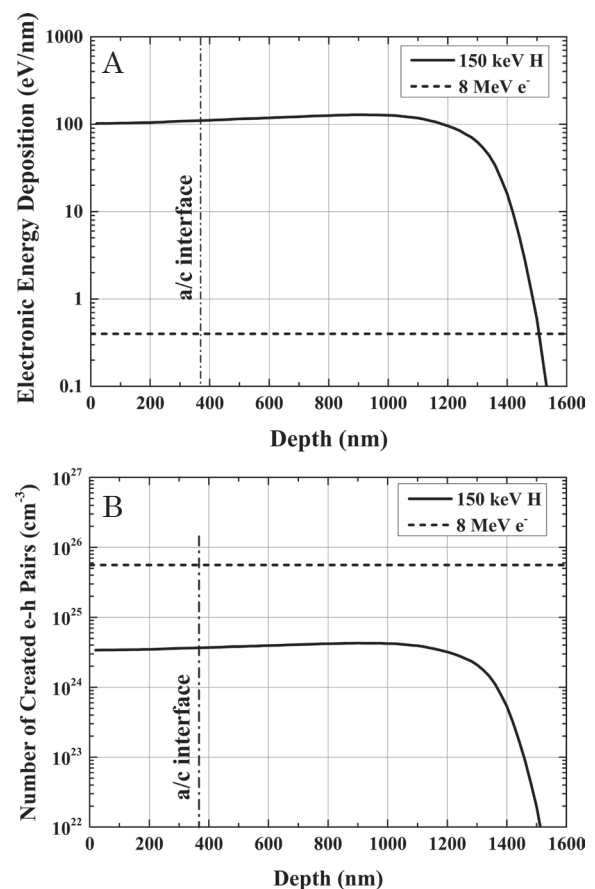


Fig. 5. electronically deposited energy (A) and the total number of created electron-hole pairs (B) from 150-keV proton ( $1 \times 10^{16}$   $\text{cm}^{-2}$ ) and 8-MeV electron ( $4.2 \times 10^{19}$   $\text{cm}^{-2}$ ) in Si.

ent defect profiles in solid materials. Secondly, the actual dpa rate was significantly different between them. Thirdly, we may be consider the H incorporation near *a/c* interface during H-IBIEC process, which probably affect the crystallization behavior. According to the previously proposed IBIEC mechanism, the crystallization rate is only dominated by the number of atomic displacements near the *a/c* interface, indicating that the rate can be scaled by nuclear stopping power<sup>7, 22, 23</sup>. However, the present results clearly suggest that another factor should be considered to demonstrate the beam-induced recrystallization processes.

## Acknowledgments

The authors would like to acknowledge Mr. T. Iha, Dr. A. Yabuuchi, and Prof. A. Kinomura for their great supports in beam irradiation experiments. We also thank to Mr. Y. Saito for his help to maintenance of experimental apparatus. This research was partly supported by a grant from the Research Institute for Integrated Science, Kanagawa University.

## References

- 1) Kool WH, Roosendaal E, Wiggers LW and Saris FW (1978) Production and beam annealing of damage in carbon implanted silicon. II. *Radiat. Eff.* **36**: 41-48.
- 2) Golecki I, Chapman GE, Lau SS, Tsaour BY and Mayr JW (1979) Ion-beam induced epitaxy of silicon. *Phys. Lett. A* **71**: 267-269.
- 3) Nakata J, Takahashi M and Kajiyama K (1981) In situ self ion beam annealing of damage in Si during high energy (0.53 MeV-2.56 MeV) As<sup>+</sup> ion implantation. *Jpn. J. Appl. Phys.* **22**: 2211-2221.
- 4) Elliman RG, Williams JS, Brown WL, Leiberich A, Maher DM and Kneol RV (1987) Ion-beam-induced crystallization and amorphization of silicon. *Nucl. Instrum. Method B* **19/20**: 435-442.
- 5) Holland OW (1989) Interaction of MeV ions with pre-existing damage in Si: A new ion beam annealing mechanism. *Appl. Phys. Lett.* **54**: 320-322.
- 6) Priolo F and Rimini E (1990) Ion-beam-induced epitaxial crystallization and amorphization in silicon. *Mater. Sci. Rep.* **5**: 319-379.
- 7) Linnros J, Holmén G and Svensson B (1985) Proportionality between ion-beam-induced epitaxial regrowth in silicon and nuclear energy deposition. *Phys. Rev. B* **32**: 2770-2777.
- 8) Williams JS, Elliman RG, Brown WL and Seidel TE (1985) Dominant influence of beam-induced interface rearrangement on solid-phase epitaxial crystallization of amorphous silicon. *Phys. Rev. Lett.* **55**: 1482-1485.
- 9) Kinomura A, Williams JS and Fujii K (1999) Mass effects on regrowth rates and activation energies of solid-phase epitaxy induced by ion beams in silicon. *Phys. Rev. B* **59**: 15214-15224.
- 10) Lulli G and Merli PG (1987) Solid-phase epitaxy of amorphous silicon induced by electron irradiation at room temperature. *Phys. Rev. B* **36**: 8038-8042.
- 11) Corbett JW and Bourgoin JC (1975) *Point Defects in Solids: Vol. 2*. Plenum, NewYork.
- 12) Lulli G and Merli PG (1993) Comparison of results and models of solid-phase epitaxial growth of implanted Si layers induced by electron- and ion-beam irradiation. *Phys. Rev. B* **47**: 14023-14031.
- 13) Hoehl D, Heera V, Bartsch H, Wollschläger K, Skorupa W and Voelskow M (1990) Temperature dependence of electron beam induced epitaxial crystallization of silicon. *Phys. Status Solidi A* **122**: K35-K37.
- 14) Nakata J (1991) Mechanism of low-temperature ( $\leq 300^\circ\text{C}$ ) crystallization and amorphization for the amorphous Si layer on the crystalline Si substrate by high-energy heavy-ion beam irradiation. *Phys. Rev. B* **43**: 14643-14668.
- 15) Nakata J (1996) Evidence of enhanced epitaxial crystallization at low temperature by inelastic electronic scattering of mega-electron-volt heavy-ion-beam irradiation. *J. Appl. Phys.* **79**: 682-698.
- 16) Sahoo PK, Mohanty T, Kanjilal D, Pradhan A and Kulkarni VN (2007) Epitaxial recrystallization of amorphous Si layers by swift heavy ions *Nucl. Instrum. Methods B* **257**: 244-248.
- 17) Sahoo PK, Som T, Kanjilal D and Kulkarni VN (2005) Swift heavy ion beam induced recrystallization of amorphous Si layers. *Nucl. Instrum. Methods B* **240**: 239-244.
- 18) Kinomura A, Yoshiie T, Chayahara A, Mokuno Y, Tsubouchi N, Horino Y, Xu Q, Sato K, Yasuda K and Ishigami R (2014) Neutron-enhanced annealing of ion-implantation induced damage in silicon heated by nuclear reactions. *Nucl. Instrum. Methods B* **334**: 48-51.
- 19) Oen OS (1973) *Cross sections for atomic displacements in solids by fast electrons*. Oak Ridge National Laboratory, Oak Ridge.
- 20) Ziegler JF, Biersack JP and Littmark U (1985) *The Stopping and Ranges of Ions in Solids*. Pergamon, New York.
- 21) Berger MJ and Seltzer SM (1982) *Stopping powers and Ranges of Electrons and Positrons*. National Bureau of Standards, Washington D.C.
- 22) Williams JS, Young IM and Conway MJ (2000) Ion beam induced epitaxy experiments in silicon under channeling and random alignments. *Nucl. Instrum. Methods B* **161-163**: 505-509.
- 23) Azevedo GdM, Williams JS, Young IM, Conway MJ and Kinomura A (2002) In situ measurements of the channeling dependence of ion-beam-induced recrystallization in silicon. *Nucl. Instrum. Methods B* **190**: 772-776.